J. Synchrotron Rad. (1998). **5**, 842–844

Activities of optical laboratories 1 and 2 at the Photon Factory

Toshiyuki Mitsuhashi,[a]* Sigenori Hiramatsu,[a] Naoya Takeuchi,[b] Masahide Itoh[b] and Toyohiko Yatagai[b]

[a]High Energy Accelerator Research Organization, 1-1 Oho, Tsukuba, Ibaraki 305, Japan, and [b]Institute of Applied Physics, University of Tsukuba, Tennodai, Tsukuba, Ibaraki 305, Japan. E-mail: mitsuhas@kekvax.ac.jp

(*Received 4 August 1997; accepted 21 October 1997*)

Recent activities at optical laboratories 1 and 2 at the Photon Factory are presented. The activities are (i) construction of optical laboratory 1, (ii) reconstruction of optical laboratory 2, (iii) construction of a visible synchrotron radiation beam extraction mirror made of beryllium, (iv) small-beam-profile measurement by means of the image restoration method, (v) application of the adaptive optical system for correction of distorted wavefronts caused by deformation of the extraction mirror, (vi) construction of a synchrotron radiation interferometer for investigation of the spatial coherency of the visible synchrotron radiation beam and its application to the measurement of vertical beam profile and size.

Keywords: accelerators; optical monitors; adaptive optics; interferometers; coherency.

1. Introduction

Optical diagnostics for accelerators using the visible part of synchrotron radiation will greatly improve the efficiency of operation of accelerators such as electron storage rings. Imaging of the synchrotron radiation will provide a visible profile of the electron beam. From the image of the electron beam, the transverse beam size can be obtained, and, with knowledge of the lattice parameters, various beam parameters such as the beam emittance and horizontal–vertical coupling can be deduced. This paper describes recent activities and developments of optical diagnostics at optical laboratories 1 and 2 at the Photon Factory.

2. Construction of optical laboratory 1 at BL27 and reconstruction of optical laboratory 2 at BL21

Optical laboratory 1 has been newly constructed at BL27 for the research and development of optical diagnostics. The laboratory consists of a class 100 clean room. The visible part of the synchrotron radiation beam is extracted by a beryllium mirror and guided into the laboratory underground by an 8 m optical pass. A spectral region from 400 to 750 nm is available, and the horizontal opening angle of the synchrotron radiation beam is 17 mrad.

The ordinary existing optical laboratory 2 at BL21 has been reconstructed. Major changes were as follows. (i) To reduce the magnetic field caused by the DC cable of the bending magnet, the wall of the laboratory room was reconstructed using 3 mm-thick iron plates. (This reconstruction is necessary to reduce the influence of the magnetic field for the streak camera.) (ii) A new room was designed to obtain a class 100 clean room.

3. Synchrotron radiation extraction mirror made of beryllium for optical laboratory 1

To reduce the wavefront error caused by surface deformation of the synchrotron radiation extraction mirror, we designed and constructed a water-cooled mirror made of beryllium (Mitsuhashi, 1995). The surface flatness of the mirror is measured by a Fizeau-type interferometer within a precision of $\lambda/20$. During the installation of the mirror in a vacuum, we applied 423 K baking. By this process, the surface of the mirror was deformed cylindrically in the horizontal by about 2.36 μm peak-to-valley, as shown in Fig. 1.

4. Small-beam-profile measurement by image restoration methods

The resolution of the beam image is mainly due to the diffraction effect including the wavefront error. To eliminate this effect, we applied the image restoration method to observe a small beam profile (Mitsuhashi & Katoh, 1996). We measured a small beam profile under ring operation at an energy of 1 GeV, 1 mA. The estimated natural emittance is 20.7 nmrad. A wavefront error caused by deformation of the Be mirror is treated as a wavefront aberration. Zernike's aberration coefficients (Born & Wolf, 1980) are evaluated from the surface deformation of the mirror by

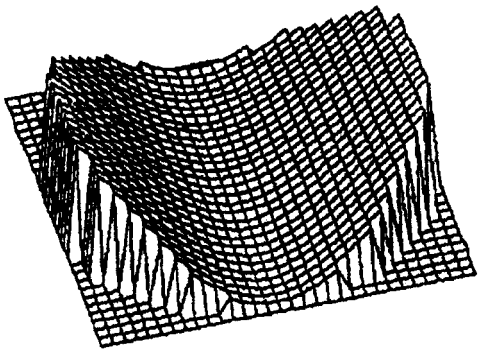

Figure 1
Surface shape of the Be mirror measured by a Fizeau-type interferometer. Peak-to-valley distance is 2.36 μm.

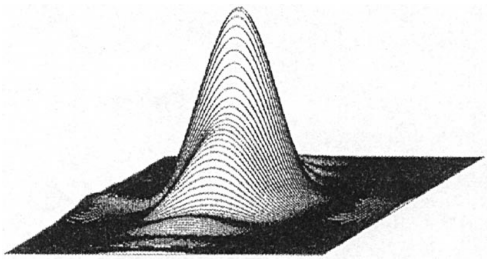

Figure 2
Point spread function (PSF) at the balanced astigmatism point. The side length of the three-dimensional plot is 730 μm.

least-square fitting of the complete Zernike power series. The point spread function (PSF) at the balanced astigmatism point is calculated by the computer code *ZEMAX* using the aberration coefficients. The resulting PSF calculated from the wavefront error is shown in Fig. 2. The r.m.s. sizes of the central peak of the PSF are 74 μm in the vertical and 81 μm in the horizontal.

In the experimental measurement of the beam profile, the focus was carefully adjusted at the balanced astigmatism point. The observed image of the beam is shown in Fig. 3(*a*). The r.m.s. beam sizes of the beam image are 96.5 μm in the vertical and 280 μm in the horizontal. To evaluate the original beam image, it is necessary to eliminate the diffraction effect. To restore the observed image, a Wiener inverse filter (Rosenfeld & Kak, 1976) was applied to the image restoration process. To perform this restoration process, we use the computer code *Hidden image* which makes use of the maximum entropy deconvolution method. The resulting restored image is shown in Fig. 3(*b*). The r.m.s. beam sizes from Fig. 3(*b*) are 49.2 μm in the vertical and 206 μm in the horizontal. Corresponding emittances are 130 pmrad in the vertical and 22 nmrad in the horizontal. The measured horizontal emittance is in good agreement with the theoretical value. The measured vertical–horizontal coupling of the emittance is 0.6%.

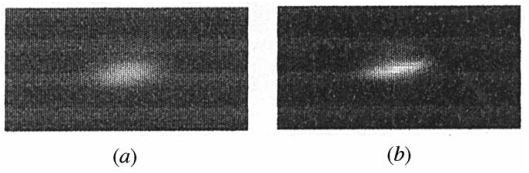

Figure 3
Beam image of the Photon Factory. The ring energy is 1 GeV and the beam current is 1 mA. (*a*) Original observed image, (*b*) image after the restoration process.

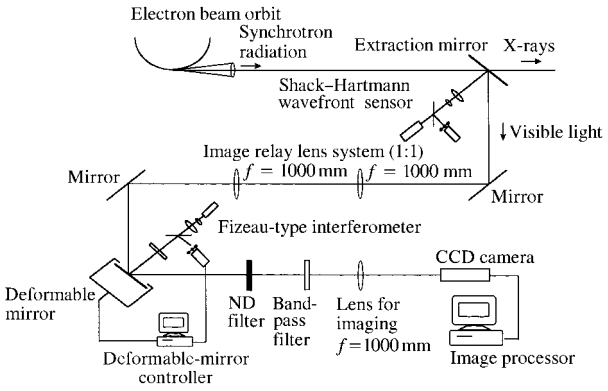

Figure 4
Layout of the adaptive optics system.

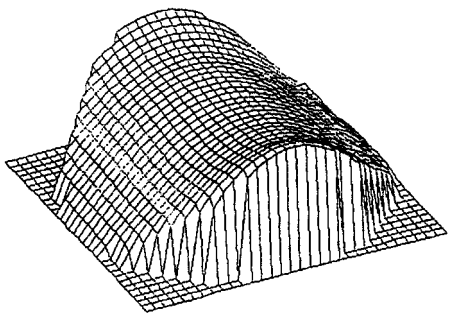

Figure 5
Shape of the deformable mirror used to cancel the wavefront error.

5. Application of adaptive optics for correcting the wavefront error caused by thermal deformation of the extraction mirror

We apply the technique of adaptive optics to eliminate the wavefront error caused by thermal deformation of the Be mirror. By using the Shack–Hartmann wavefront sensor (Takeuchi *et al.*, 1997*a*), we can measure the mean surface of the wavefront error free from the floor vibration. We constructed the Shack–Hartmann wavefront sensor; it consists of a multi-lens array (8 × 8 array, 250 μm pitch, 4.5 mm focal length), a beam expander (20:1), an image relay lens system (1:1), an He–Ne laser having a collimator system and a digital CCD camera. The layout of the adaptive optical system applied for the optical diagnostics beamline is shown in Fig. 4 (Takeuchi *et al.*, 1997*b*). A deformable mirror is set in the conjugated plane of the Be mirror. The wavefront error on the Be mirror is transferred onto the deformable mirror using a 1:1 relay lens system and compensated by the deformable mirror. We used the deformable mirror CILAS BIM31, which is a 'bimorph'-type mirror. It is equipped with 31 electrodes that can be separately driven by 400 V. The shape of the deformable mirror is just the opposite shape of the wavefront error, as shown in Fig. 5. The subtraction between the two wavefronts is less than λ/5.6 in r.m.s. The performance of the adaptive optical system will be tested with a synchrotron radiation beam in the next operation at the Photon Factory ring.

6. Synchrotron radiation interferometer for investigation of the spatial coherence of visible synchrotron radiation and its application to the vertical beam profile

The principle of object-profile measurement by means of the spatial coherence of light is known as van Citterut–Zernike's theorem (Born & Wolf, 1980). We applied this principle to measure the vertical beam profile of the beam (Mitsuhashi, 1997).

A synchrotron radiation interferometer, which is basically a two-beam interferometer of the wavefront division type, was designed and constructed by using polarized quasi-monochromatic rays. A schematic drawing of the interferometer is shown

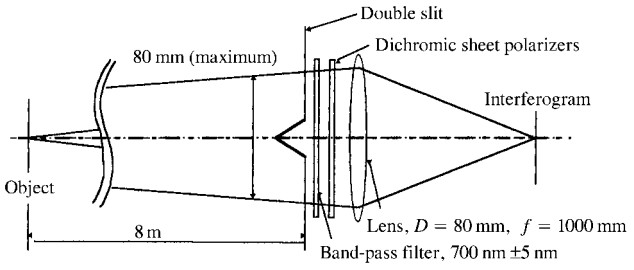

Figure 6
Schematic drawing of the interferometer.

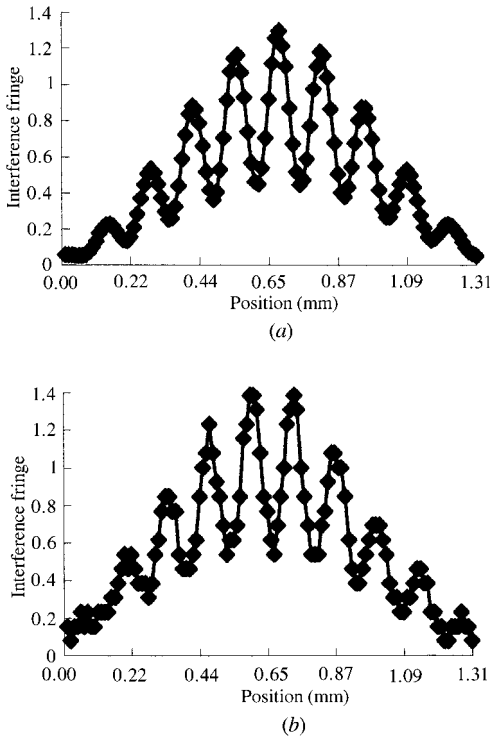

Figure 7
Observed interferograms by (*a*) σ-polarized component, (*b*) π-polarized component.

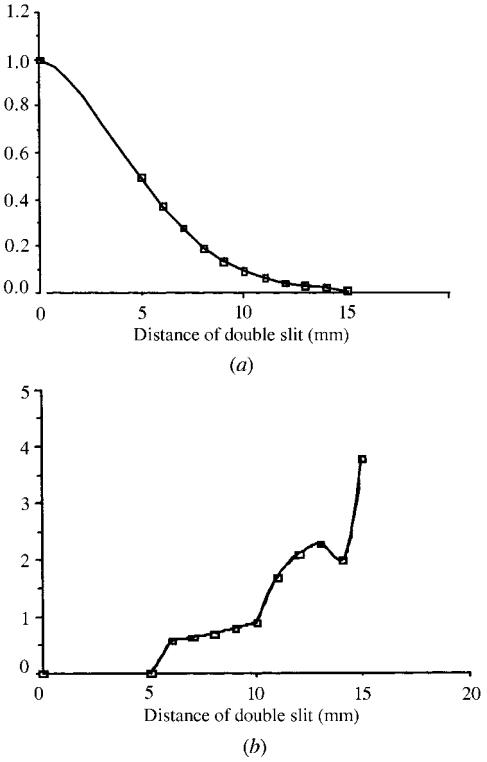

Figure 8
Observed complex degree of spatial coherence: (*a*) absolute value (visibility), (*b*) phase (units of the *y* axis are radians).

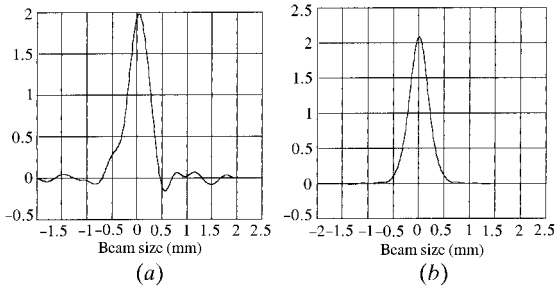

Figure 9
The beam profile obtained by a Fourier transform: (*a*) complete Fourier transform, (*b*) Fourier cosine transform.

in Fig. 6. In the vertical plane, the elliptical polarity of the synchrotron radiation is opposite the medium plane of the electron beam orbit. Therefore, one can expect a phase difference of π in the interferograms corresponding to σ- and π-polarized components. Observed interferograms (λ = 700 nm) corresponding to σ- and π-polarized components are shown in Figs. 7(*a*) and 7(*b*). Comparing these two interferograms, it can be seen that there is a phase difference of π between them, as expected.

The absolute value (visibility) and the phase of the complex degree of spatial coherence were measured by changing the distance of the double slits from 5 to 15 mm under a ring operation of 2.5 GeV and 2 mA. The results are shown in Figs. 8(*a*) and 8(*b*). For this measurement, one (σ) of the polarized components was selected. By means of van Citterut–Zernike's theorem, the vertical beam profile is obtained by the Fourier transform of the complex degree of spatial coherence. The resulting beam profile is shown in Fig. 9(*a*). Due to the phase term of the complex degree of spatial coherence, the beam profile has an asymmetric distribution. This asymmetry in the profile was mainly caused by a deformation of the Be extraction mirror. As in the similar technique of noise-elimination processing for the electric signals, it is possible to eliminate an asymmetric part of the Fourier components of the complex degree of spatial coherence. As an easy way, we tried to neglect the Fourier sine terms. The result is shown in Fig. 9(*b*). The r.m.s. beam size in Fig. 9(*b*) is 202 µm. This technique is very useful for eliminating unknown effects (asymmetric terms of the wavefront aberrations) of the optical components between the object beam and image plane.

References

Born, M. & Wolf, E. (1980). *Principle of Optics*. Oxford: Pergamon.
Mitsuhashi, T. (1995). *Proc. 10th Symp. Accel. Sci. Technol.*, pp. 275–277. Japan Synchrotron Radiation Research Institute.
Mitsuhashi, T. (1997). *Proc. 1997 Part. Accel. Conf.* To be published.
Mitsuhashi, T. & Katoh, M. (1996). *Proc. 5th Eur. Part. Accel. Conf.* Bristol: Institute of Physics.
Rosenfeld, A. & Kak, A. C. (1976). *Digital Picture Processing*. New York: Academic Press.
Takeuchi, N., Mitsuhashi, T., Itoh, M. & Yatagai, T. (1997*a*). *Technical Digest*, Vol. 13, *Nonastronomical Adaptive Optics* (NAAO '97), pp. 26–28. Optical Society of America.
Takeuchi, N., Mitsuhashi, T., Itoh, M. & Yatagai, T. (1997*b*). *Proc. 1997 Part. Accel. Conf.* To be published.